CIRP Annals - Manufacturing Technology 60 (2011) 271–274

Contents lists available at ScienceDirect

CIRP Annals - Manufacturing Technology

journal homepage: http://ees.elsevier.com/cirp/default.asp

BioCell Printing: Integrated automated assembly system for tissue engineering constructs

P. Bartolo (2)[a,*], M. Domingos [a], A. Gloria [b], J. Ciurana [c]

[a] *Centre for Rapid and Sustainable Product Development, Polytechnic Institute of Leiria (IPL), Leiria, Portugal*
[b] *Institute of Composite and Biomedical Materials, National Research Council, Piazzale Tecchio 80, 80125 Naples, Italy*
[c] *Universitat de Girona, Spain*

ARTICLE INFO

Keywords:
Biomedical
Extrusion
Rapid prototyping

ABSTRACT

The production methodology of 3D constructs for tissue regeneration is usually a complex discontinuous process involving three different stages: (1) production of 3D matrices; (2) matrix sterilisation and cell seeding; (3) *in vitro* dynamic cell culture. This paper presents a novel automated bench-top manufacturing system called *BioCell Printing*, designed for the integrated, continuous and fully automated production and *in vitro* dynamic culture of tissue engineering constructs. The BioCell aims at the rapid production of tissue-engineered substitutes with low risk of contamination, increasing the chances of direct clinical application.

1. Introduction

Tissue engineering (TE), often called regenerative medicine and reparative medicine, is an interdisciplinary field combining efforts from cell biologists, engineers, material scientists, mathematicians, geneticists, and clinicians towards the development of biological substitutes that restore, maintain, or improve tissue function [1]. It is a rapidly expanding area addressing the organ shortage problem that comprises tissue regeneration and organ substitution. The most promising approach for tissue engineering involves the seeding of porous, biocompatible/biodegradable three-dimensional (3D) scaffolds, with donor cells to promote tissue regeneration. Most of the human cell types are anchorage dependent, so scaffolds play a major role in this process, both *in vitro* as *in vivo* representing the initial biomechanical support for cell attachment, differentiation and proliferation. The capability to deliver and retain cells and growth factors, enhance the diffusion of cell nutrients, oxygen and vascularisation are critical aspects for a successful organized tissue regeneration process [1].

It is very complex, if not impossible, to establish an ideal scaffold definition, even for a single tissue type due to the functional multitude of the tissues [2]. The considerations are complex and include chemical, morphological, mechanical and biological factors and their mutability with time. Nonetheless, there is a general agreement regarding some of the major requirements, namely, biocompatibility, biodegradability, appropriate porosity, micro- and macro-structure, pore size and shape, mechanical strength, adequate surface finish, surface topography, easily manufactured and sterilised [1].

Additive fabrication processes represent a new group of non-conventional fabrication techniques recently introduced in the biomedical field [3]. In TE, additive fabrication processes are used to produce scaffolds with customised external shape and predefined internal morphology, allowing good control of pore size and pore distribution. The various additive fabrication technologies for TE include stereolithographic processes [4], laser sintering [5], extrusion [6] and 3DP technologies [7]. Recently, some authors have suggested "bioprinting systems" as a novel methodology for the fabrication of 3D biological structures through the computer-aided deposition of cells, cell aggregates and biomaterials [8]. Commercially available inkjet printers were successfully redesigned [9] or new ones specifically engineered [10] to guide biological assembly following a CAD template. These self-assembly and "scaffold-less" approaches are emergent in TE, demonstrating that fully biological tissues can be engineered with specific compositions and shapes, by exploiting cell–cell adhesion and the ability of cultured cells to grow their own extra cellular matrix (ECM), without the employment of synthetic materials, thus reducing the possible inflammatory responses owing to the interaction between biological and non-biological materials.

The production of 3D constructs for tissue regeneration is a complex process involving different stages. The first stage involves the production of 3D matrices with/without embedded cells, either using conventional or non-conventional techniques. The matrices are then sterilised and prepared for manual cell seeding or directly implanted into the body. Depending on the adopted strategy, a final stage of *in vitro* dynamic culture of the matrix-cells system may be required and different types of bioreactors can be used. One of the major drawbacks of this

* Corresponding author. Tel.: +351 244 569 441; fax: +351 244 569 444.
E-mail address: pbartolo@ipleiria.pt (P. Bartolo).

0007-8506/$ – see front matter © 2011 CIRP.
doi:10.1016/j.cirp.2011.03.116

Fig. 1. *BioCell Printing* device: (a) CAD model; (b) functional prototype.

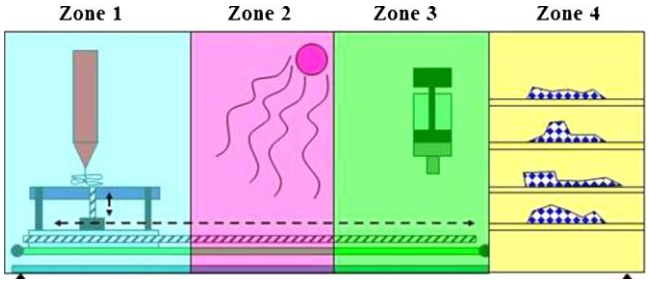

Fig. 2. Schematic representation of BioCell assembly device.

approach is the risk of contamination of the 3D constructs associated with their transference between the different stages, due to the reduced sterilisation conditions inherent to the process. Moreover, the different stages of the process are not fully integrated and cannot be performed in a continuous and sequential manner which significantly increases the production time, and decreases the chances for direct clinical application.

This paper explores a novel fabrication route for TE through the integration of the abovementioned stages in a fully automated bench-top manufacturing system called *BioCell Printing*. The capability of the system to produce polymer-based scaffolds for TE applications is evaluated. Poly(ε-caprolactone) (PCL) is selected to generate 3D scaffolds with different architectures and morphological, mechanical and biological tests are performed.

1.1. BioCell Printing

The *BioCell Printing* is a novel assembly fabrication system enabling the integration and synchronization of the different stages of production and culture of 3D matrices with reduced manual intervention (Fig. 1).

3D constructs with or without embedded cells are produced in Zone 1 through a multiple-head bioprinter as illustrated in Fig. 2. Depending on the chosen strategy, acellular or cellular scaffolds, a precision robotic arm then transfers the 3D constructs to Zone 2, where they are sterilised by chemical (ethylene oxide or supercritical CO_2) or physical processes (UV, β and γ radiation). After sterilisation, scaffolds are homogeneously seeded with cells using a robotic dispenser in Zone 3. Finally, 3D constructs with embedded or seeded cells are cultured *in vitro* under dynamic conditions using a bioreactor.

Optimal conditions of sterilisation, humidity, temperature and % of CO_2 are maintained during all process by the incorporation of an incubating chamber.

A dynamic integrated computational platform for information management, called BIOMAS was developed in Matlab to ease the project coordination between different users, and to control the four zones of the *BioCell Printing* system.

Table 1 presents the main parameters that control Zone 1 of the *BioCell Printing* with a direct influence in the morphological and biomechanical properties of the extruded structures

Table 1
Process-instrument-design parameters.

Process parameters	Instruments parameter	Design parameters
Deposition velocity Layer thickness	Liquefier temperature Extrusion velocity Nozzle tip size	Filament distance Lay-down pattern

Table 2
Process conditions adopted for Zone 1.

Process conditions	
Deposition velocity	7 mm/s
Layer thickness	0.28 mm
Liquefier temperature	80 °C
Extrusion velocity	84 rpm
Nozzle tip size	0.3 mm
Filament distance	0.650
Lay-down pattern	0/90° and 0/45°

2. Materials and methods

2.1. Materials

Poly(ε-caprolactone) (CAPA 6500, M_w = 50,000) in the form of pellets was obtained from Perstorp Caprolactones (Cheshire, United Kingdom).

2.2. Scaffolds design and fabrication

Rectangular prisms measuring 30 mm (length) × 30 mm (width) × 8 mm (height), were initially designed using UNIGRAPHICS NX software (Siemens PLM Software, Portugal). The STL file format was then transferred to the BIOMAS platform, where it was automatically sliced into a number of 2D layers of pre-defined thickness. The process conditions adopted to obtain highly porous scaffolds with a fully interconnected pore network are indicated in Table 2.

2.3. Scaffold morphology

The morphological analyses of the 3D structures were carried out using a scanning electron microscope (SEM, FEI Quanta 600F) and micro-computed tomography (μCT), both to visualize and evaluate the physical integrity of the material filaments and layers and to understand if the previously defined pore geometry and size were maintained during the fabrication process.

μCT was performed through a SkyScan 1072 (Aartselaar, Belgium) system using a rotational step of 0.9° over an angle of 180°. Cross-sections and 3D model of PCL scaffolds were reconstructed using both SkyScan's software package, Image J software and Mimics (Materialise). μCT analysis allowed to evaluate interesting scaffold characteristics, such as porosity, surface area to volume ratio, and interconnectivity (Table 3).

Table 3
Interesting scaffold characteristics: porosity, surface area to volume ratio, and interconnectivity [11].

Characteristics	Formulae/definition
Porosity	100% × volume of pores/sum of volume of pores and scaffold material
Surface area to volume ratio	Surface area of scaffold struts volume of scaffold material
Interconnectivity	100% × volume of interconnected pores volume sum of interconnected and closed pores

2.4. Mechanical analysis

Compression tests were performed on the 3D scaffolds to evaluate its mechanical properties. Each block-shaped specimen was characterized by a length (l) of 5.0 mm, a width (w) of 5.0 mm and a height (h_0) of about 8 mm. All tests were carried out on scaffolds in dry state at a rate of 1 mm/min up to a strain value of 0.5 mm/mm, using an INSTRON 5566 testing system. The "apparent" stress is evaluated as a force F measured by the load cell divided by the total area of the apparent cross-section of the scaffold:

$$\sigma = \frac{F}{A} \quad (1)$$

with ($A = l.w$). Strain ε is defined as the ratio between the scaffold height variation Δh (i.e., the vertical displacement equal to the crosshead displacement) and the scaffold initial height h_0:

$$\varepsilon = \frac{\Delta h}{h_0} \quad (2)$$

2.5. Biological analysis

3D scaffolds (5 mm × 5 mm × 3.36 mm) and 0/90° lay-down pattern were seeded with human osteoblast-like cells (MG-63) using a density of 17×10^3 cells/sample. Cell viability and proliferation were then evaluated by using the Alamar Blue assay.

The number of viable cells is correlated with the magnitude of dye reduction and expressed as a percentage of Alamar Blue reduction.

PCL scaffolds were also seeded with human mesenchymal stem cells (hMSCs) to qualitatively investigate cell adhesion and spreading after 72 h, through confocal analysis using phalloidin. A confocal laser scanning microscope Zeiss LSM 510/ConfoCor 2 was used.

3. Results and discussion

A morphological evaluation of the structures was carried out under SEM. The scaffolds produced with the *BioCell Printing* adopting two different lay-down patterns, 0/90° and 0/45°, present a well-defined internal geometry with square and complex polygonal pores shapes, respectively (Fig. 3). The structures are characterized by fully interconnected pores of regular dimensions (~350 μm × 350 μm) and uniform distribution. The extruded filaments show a regular circular geometry with ~300 μm diameter, according to the nozzle tip used (300 μm), as well a good adhesion between adjacent layers, as illustrated in Fig. 3b and d.

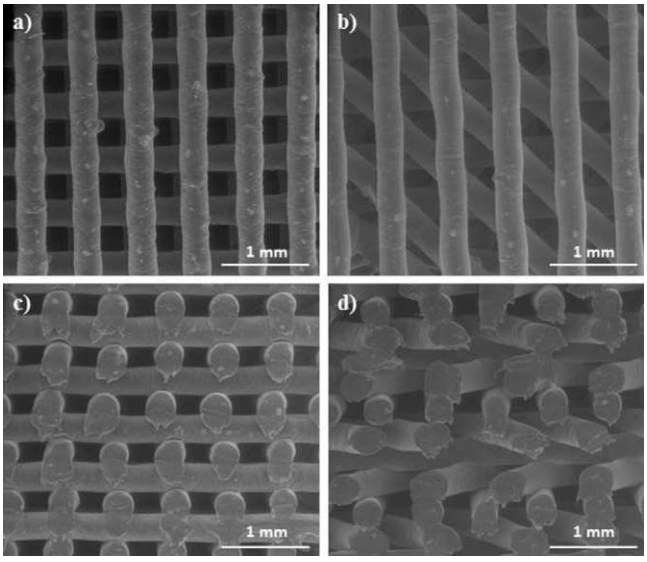

Fig. 3. SEM micrographs of 3D scaffolds: (a) 0/90° lay-down pattern top view; (b) 0/45° lay-down pattern top view; (c) 0/90° lay-down pattern cross-section view; (d) 0/45° lay-down pattern cross-section view.

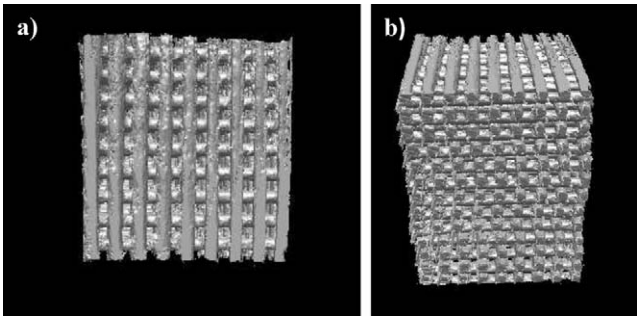

Fig. 4. 3D reconstructions obtained from μCT analysis on PCL scaffolds with a 0/90° lay down pattern and a filament distance of 650 μm: (a) top view; (b) lateral view.

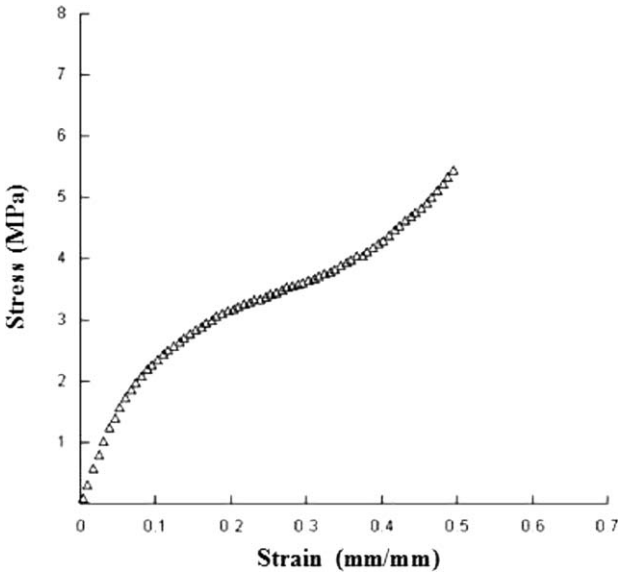

Fig. 5. Typical stress–strain curve obtained for 3D scaffolds characterized by a 0/90° lay-down pattern and a filament distance of 650 μm, compressed at a rate of 1 mm/min up to a strain value of 0.5 mm/mm.

The μCT analysis confirmed that well-organized PCL scaffolds can be obtained, showing precise pore size and shape, and a repeatable micro-structure (Fig. 4).

The μCT tests showed a good consistency between real and theoretical values regarding filament diameter and pore size. In particular, this analysis showed a mean fiber diameter of 300 μm and a centre-to-centre filament distance of 650 μm between two filaments in the same layer. Scaffold interconnectivity (100%), surface area to volume ratio (20.07 mm^2/mm^3) and porosity (60%) were also measured.

Compression tests suggest that the 3D scaffold mechanical behaviour is similar to that of flexible foam [12]. A linear region is well defined at low values of strain, suggesting an initial stiff mechanical response. This zone is followed by a region with lower

Table 4
Mechanical properties of 3D scaffolds with different lay-down patterns.

Lay-down pattern	Compressive modulus E (MPa)	Maximum stress σ_{max} (MPa)
0/45°	19.1 ± 2.8	4.9 ± 0.3
0/90°	34.2 ± 3.8	5.6 ± 0.2

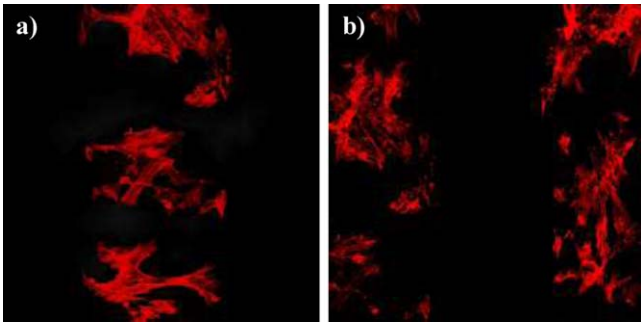

Fig. 6. Results from confocal analysis on cell-scaffold constructs: images related to a filament (a) and two filaments (b) of the 3D PCL scaffolds.

stiffness. It can also be noticed another stiff portion of the stress–strain curve (Fig. 5).

The influence of lay-down pattern on the mechanical behaviour of scaffolds is presented in Table 4.

According to Table 4, an angle reduction between filaments decreases the mechanical properties of the scaffolds. These results are in agreement with previous works performed by the authors with PCL and other additive fabrication systems [13]. The scaffolds show low cytotoxicity and can be used for TE applications as observed through the Alamar Blue assay. Tests carried out after 7 and 14 days show an increase in cell proliferation, confirmed by the Alamar Blue reduction values ($13.53 \pm 0.76\%$ at 7 days and $49.32 \pm 12.12\%$ at 14 days).

Furthermore, confocal analysis confirms the excellent biological characteristics of these scaffolds showing a high level of hMSC adhesion and spreading after 72 h of cell seeding, as illustrated in Fig. 6. This figure clearly highlights the phalloidin-labelled actin filaments, confirming a good cell viability.

4. Conclusions

A novel integrated automated assembly system for TE, called *BioCell Printing*, is presented, enabling the fabrication of 3D scaffolds with good reproducibility, structural stability and tuneable morphological/mechanical properties. To validate the system scaffolds were produced with different topologies. The scaffolds present well-defined architecture and pores, and a fully interconnected pore structure. The mechanical properties, which depend on the architecture of the scaffold, present elastic modulus values that enable the use of these scaffolds for bone tissue regeneration. Biological tests suggest a good cell adhesion and proliferation of both hMSCs and osteoblast-like cells. Preliminary results show that the *BioCell Printing* system is an innovative fabrication approach and a viable technique for TE. Further investigations will be carried out in order to fully explore the capability of the *BioCell Printing* to produce multiple-material 3D cell laden constructs that can be applied as biomimetic substitutes for zonal cartilage regeneration.

References

[1] Bártolo PJ, Almeida HA, Rezende RA, Laoui T, Bidanda B (2008) *Advanced Processes to Fabricate Scaffolds for Tissue Engineering, Virtual Prototyping & Bio-manufacturing in Medical Applications*. Springer.
[2] Hutmacher DW, Schantz JT, Lam CXF, Tan KC, Lim TC (2007) State of the Art and Future Directions of Scaffold-based Bone Engineering from a Biomaterials Perspective. *Journal of Tissue Engineering and Regenerative Medicine* 1:245–260.
[3] Bartolo PJ, Gaspar J (2008) Metal Filled Resin for Stereolithography Metal Part. *CIRP Annals—Manufacturing Technology* 57:235–238.
[4] Melchels FPW, Feijen J, Grijpma DW (2009) A Poly(D,L-lactide) Resin for the Preparation of Tissue Engineering Scaffolds by Stereolithography. *Biomaterials* 30:3801–3809.
[5] Kruth J-P, Levy G, Klocke F, Childs THC (2007) Consolidation Phenomena in Laser and Powder-bed Based Layered Manufacturing. *CIRP Annals—Manufacturing Technology* 56:730–759.
[6] Hoque ME, Wong YS, Feng W, Li S, Huang MH, Vert M, Hutmacher DW (2009) Processing of PCL and PCL-based Copolymers into 3D Scaffolds, and Their Cellular Responses. *Tissue Engineering Part A* 15:3013–3024.
[7] Dimitrov D, Schreve K, de Beer N (2006) Advances in Three Dimensional Printing—State of the Art and Future Perspectives. *Rapid Prototyping Journal* 12:136–147.
[8] Mironov V, Boland T, Trusk T, Forgacs G, Markwald RR (2003) Organ Printing: Computer-aided Jet-based 3D Tissue Engineering. *Trends in Biotechnology* 21:157–161.
[9] Nakamura M, Kobayashi A, Takagi F, Watanabe A, Hiruma Y, Ohuchi K, Iwasaki Y, Horie M, Morita I, Takatani S (2006) Biocompatible Inkjet Printing Technique for Designed Seeding of Individual Living Cells. *Tissue Engineering* 11:1658–1666.
[10] Saunders RE, Gough JE, Derby B (2008) Delivery of Human Fibroblast Cells by Piezoelectric Drop-on-demand Inkjet Printing. *Biomaterials* 29:193–203.
[11] Ho ST, Hutmacher DW (2006) A Comparison of Micro CT with Other Techniques Used in the Characterization of Scaffolds. *Biomaterials* 27:1362–1376.
[12] Kyriakidou K, Lucarini G, Zizzi A, Salvolini E, Belmonte MM, Mollica F, Gloria A, Ambrosio L (2008) Dynamic Co-seeding of Osteoblast and Endothelial Cells on 3D Polycaprolactone Scaffolds for Enhanced Bone Tissue Engineering. *Journal of Bioactive and Compatible Polymers* 23:227–243.
[13] Domingos M, Chiellini F, Gloria A, Ambrosio L, Bartolo PJ, Chiellini E (2009) BioExtruder: Study of the Influence of Process Parameters on PCL Scaffolds Properties. in Bartolo PJ, (Ed.) *Innovative Developments in Design and Manufacturing—Advanced Research in Virtual and Rapid Prototyping*. CRC Press/Taylor & Francis, pp. 67–73.